CRAB CAVITIES FOR THE LHC UPGRADE

Rama Calaga, CERN, Geneva, Switzerland

Abstract

The talk will review the motivation and the evolution of the crab cavity technology for luminosity enhancement and leveling for the HL-LHC upgrade project. The present status and the foreseen roadmap for the crab-cavity system is also presented.

INTRODUCTION

Controlled experiments to assess the effect of the parasitic interactions as a function of crossing angle indicate that the present separation of approximately 10σ in the common regions of the interaction regions is required [1]. For this experiment, a 50 ns bunch spacing with 36 bunches and 2 head-on collisions at IP1 and IP5 with 8-16 long-range interactions per IP were used. The separation between the two beams, first in IP1, and then in IP5 were reduced systematically via the crossing angle. Figure 3 shows the total bunch-by-bunch losses as a function of reduced separation only for IP1. The baseline losses are indicated by the 12 non-colliding bunches at the bottom. From

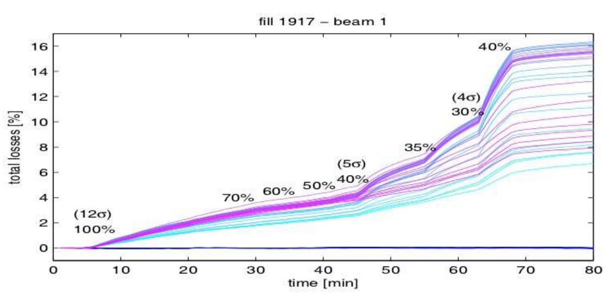

Figure 1: Bunch-by-bunch losses for beam 1 with controlled reduction of crossing angle at IR1.

this experiment, it can be concluded that the bunches with the most number of long-range interactions suffer the highest losses and the onset of steep losses start approximately at 5σ. The increase in losses can be interpreted as the reduction in dynamic aperture as a function of the increased long-range effects [1].

Some relevant parameters for the LHC design and upgrade are listed in Table 1. For the nominal design and foreseen upgrade parameters, the maximum number of long-range interactions reach a maximum of 120 or more. Therefore, a sufficiently large crossing angle leading to an approximate separation of 10σ becomes inevitable.

Table 1: Some relevant parameters for the LHC nominal and upgrade lattices.

	Unit	Nominal	Upgrade
Energy	[TeV]	3.5-7	7
p/bunch	[10^{11}]	1.15	1.7-2.0
Bunch Spacing	[ns]	50-25	25
ϵ_n (x,y)	[μm]	2.5	2.5-3.75
σ_z (rms)	[cm]	7.55	7.55
IP$_{1,5}$ β^*	[cm]	55-100	15-25
Betatron Tunes	-	{64.31, 59.32}	
X-Angle: $2\phi_c$	[μrad]	250-315	470-580
Piwinski Angle	$\frac{\sigma_z}{\sigma^*}\phi_c$	$\leq$0.7	$\geq$2.5
Main/Crab RF	[MHz]	400	
Peak luminosity	[$10^{34}\ cm^{-2}s^{-1}$]	1.0	20

CROSSING ANGLE

The consequence of the increased crossing angle is a reduction of the potential luminosity (see Fig. 2) compared to that of a pure head-on collision.

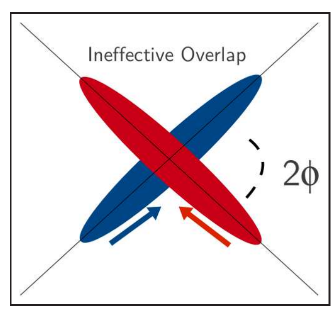

Figure 2: Schematic of the bunch crossing to illustrate the inefficient overlap.

The effective luminosity with a crossing angle can be conveniently represented as a Piwinski reduction factor R_Φ given by

$$R_\Phi = \frac{1}{\sqrt{1+\Phi^2}}. \tag{1}$$

Here, $\Phi = \frac{\sigma_z}{\sigma_x^*}\phi$ and ϕ is the half crossing angle. This reduction can alternately be illustrated as an increase in the effective transverse size given by

$$\sigma_{eff} = \sqrt{\sigma_x^2 + \sigma_z^2\phi^2} \tag{2}$$

The reduction factors for present LHC and some foreseen upgrade parameters are listed in Table 2. Note that the crossing angles were calculated using $\phi = d\sqrt{\epsilon/\beta^*}$ with $d = 10\sigma$ as a minimum separation for comparison purposes. The actual operational crossing angles maybe empirically adjusted to minimize losses.

Table 2: Piwinski reduction factors calculated for the present LHC and some foreseen upgrade paramaters

	2011-12	after LS1	after LS3
Energy [Tev]	3.5-4.0	7.0	7.0
β^* [cm]	60-100	55	15
$2\phi_c$ [μrad]	260-313	247	473
R$_\Phi$ ($\sigma_z = 7.55$cm)	0.85-0.94	0.82	0.37
R$_\Phi$ ($\sigma_z = 7.55$cm)	0.74-0.76	0.74	0.28

For upgrade paramaters using $d \approx 10\sigma$ lead to a significantly larger and distorted footprints compared to that of the nominal design as seen in Fig. 3. For the footprint calculations, two head-on and 21 long-range interations per IP were used. Although, the footprint alone is not a quantitative figure for beam lifetime, a footprint similar to one shown in Fig. **??** is not an effective starting point. To recuperate a qualitatively similar footprint as the nominal, a separation of 12σ has to be used [2]. The consequence is a reduced peak luminosity (approximately an additional 16%). Synchro-betatron resonances might become important as the Piwinski angles for the upgrade parameters reach beyond 2.

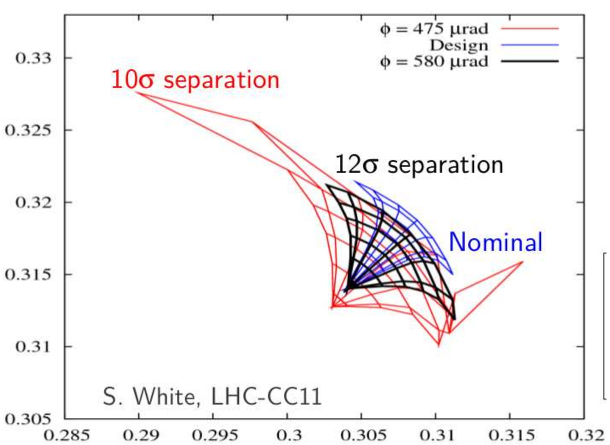

Figure 3: Footprints calculated for nominal and upgrade parameters with 10σ and 12σ beam separation with head-on collisions at 2 IPs and 16 or more long-range interactions per IP.

CRAB SCHEME AND SPECIFICATIONS

To recover the overlap, two deflecting cavities in a "crabbing" phase can be employed (see Fig. 4) as was originally proposed by R. Palmer for a geometric compensation for linear colliders [3].

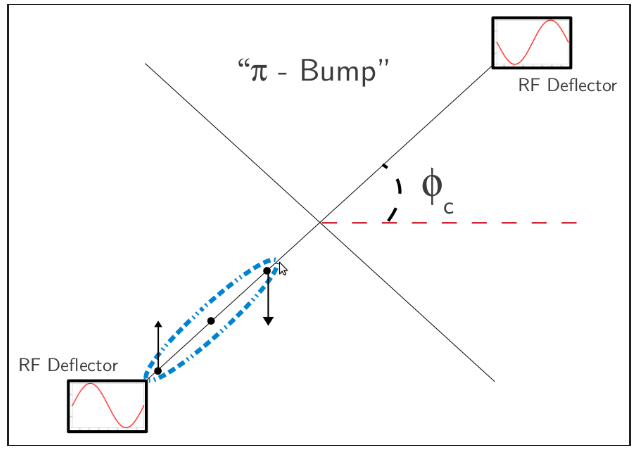

Figure 4: Schematic of the local crab crossing across the interaction region using a pair of deflecting cavities.

The transverse kick imparted to the bunch is given by

$$\Delta p_x = \frac{qV_c}{E_b}\sin\left(\phi_s + kz\right) \tag{3}$$

where V_c is the cavity voltage, E$_b$ is the beam energy, ϕ_s is the synchronous phase, k is the wave number (ω_{RF}/c) and z is the offset of the particle within the bunch w.r.t to the synchronous particle. This kick results in a transverse displacement ($x = R_{12}x'$) at the IP of the head and the tail of the bunch so as to provide head-on collisions.

Cavity Voltage

The required cavity voltage can be deduced and is given by

$$V_c = \frac{2cE_b\tan\left(\phi_c\right)}{\omega_{RF}R_{12}}\frac{\sin\left(\pi Q\right)}{\cos\left(\psi^x_{cc\to ip} - \pi Q\right)} \tag{4}$$

where ω_{RF} is the RF frequency, $R_{12} = \sqrt{\beta_{crab}\beta^*}$ which are the lattice functions at crab cavity and IP respectively, $\psi^x_{cc\to ip}$ is the phase advance from the cavity to the IP. Based on two different transfer matrix components (R_{12}) the required voltage as a function of full crossing angle is shown in Fig. 5. The crossing angles for the present and upgrade scenarios are marked with arrows for illustration. Using am optimistic $R_{12} = 30m$ and preserving the present transverse emittances of 2.5μm in the LHC, a 6 MV cavity voltage per side of the IP for each beam would be sufficient.

This voltage can be realized with two cavities operating at 3 MV. With 3 MV/cavity, there remains a substantial margin (see Table 3) for the cavity surface fields before they reach upper limits commonly accepted SRF community (60 MV/m and 100 mT). If a more conservative $R_{12} = 25m$ and larger transverse emittances are used, then the required cavity voltage increases to approximately 10

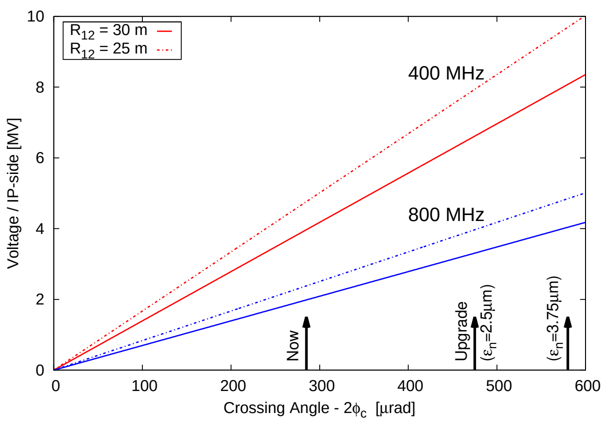

Figure 5: Required cavity voltage as a function of full crossing angle $2\phi_c$. Some labels are included to identify the different states of the LHC.

MV (see also Ref. [4]). This entails an additional cavity to make up the difference. A minimum set of two cavities is the desired option from technological, impedance, safety and operational considerations.

Frequency Choice

Ideally, the highest possible frequency is desirable due to space constraints, voltage and phase noise dependence on the frequency. However, due to the rather long proton bunches in the LHC, a low frequency cavity is preferred to minimize the longitudinal RF curvature. For example, Fig. 6 shows the effect of an 800 MHz cavity on the colliding proton bunches in the LHC.

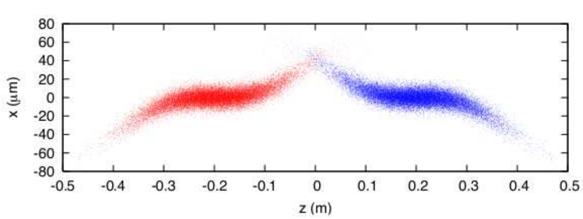

Figure 6: Effect of the RF curvature on the colliding proton bunches with an 800 MHz crab cavity (courtesy K. Ohmi).

The the RF curvature can represented as an additional reduction factor in the luminosity equation which has been analytically and numerically studied in detail [5]. This reduction factor is approximately 1 for a frequency of 400 MHz for a wide range of β^* as opposed to a 800 MHz cavity. Therefore, a 400 MHz crab cavity frequency is most suitable assuming cavities with a small footprint compatible with the LHC IR constraints can be realized at this frequency. The baseline operating temperature is chosen to be 2K due to cavity performance, microphonics and safety margin. It should be noted that at 400 MHz, the option to operate at higher temperatures like 4.5K also remains possible. The main RF frequency is 400 MHz thus leading to operation ease with the same frequency for the crab cavities.

RF Power

Due to "zero" beam-loading in the crabbing phase and the extremely low losses in an SRF cavity, only a minimum RF power is required to keep the cavity field stable. This minimum power is primarily determined by the detuning due to microphonics or phase jitter. If the beam trajectory in the cavity deviates from the electrical (or magnetic) center, additional RF power will be needed to compensate the beam loading depending on the offset. The beam induced voltage is linearly proportional to the transverse offset and is given by

$$V_b = Q_L I_b \frac{R_\perp}{Q}(k\Delta x). \tag{5}$$

Fig. 7 shows the input power as a function of coupling factor expressed in Q_{ext}.

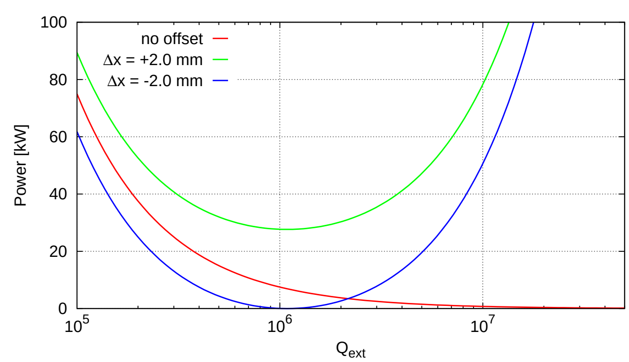

Figure 7: Required RF input power to maintain stable field in the cavity as a function of Q_{ext} for zero, positive and negative beam loading.

At 3 MV operating voltage per cavity and a $Q_{ext} = 10^6$, the minimum RF power required is approximately 8kW. For beam offsets of 2 mm, the required power can reach upto 30 kW. Assuming a safety factor of 2, the input amplifiers requirements can be set at 60 kW. This also allows additional power required for RF processing of cavities.

Since, the required power is rather modest (60 kW), a simplified version of the LHC coupler [6] adapted to the beam ports of the crab cavities can be employed. The modest power also allows for the use of Tetrodes, IOTs or solid state input amplifiers. All three options should yield an improved amplitude and phase noise performance compared to the equivalent klystrons.

CAVITY GEOMETRY

Pillbox Cavity

The standard solution for a deflecting or crabbing cavity is to employ a pillbox cavity operating on the TM_{110} (see Fig. 8), quite appropriate and widely used in $\beta = 1$ accelerators. The deflecting or crabbing mode is generally a higher order mode. In such cavities, the transverse dimen-

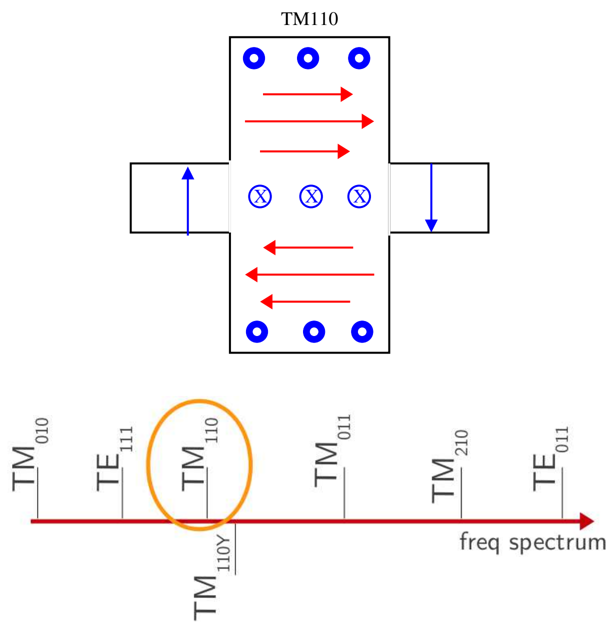

Figure 8: Top: Schematic of a pillbox cavity operating on TM_{110} mode to provide transverse deflection. Bottom: Schematic of first few modes in a pillbox cavity.

sions typically scale inversely with the frequency. Addtionally, the cavities would nominally have an elliptical profile with the semi-major axis in the direction of the deflection. For example, a 400 MHz cavity would have an approximate radius of 610 mm and an 800 MHz cavity would be about half that value (305 mm). It should be noted that the LHC beam pipes from their centers are only separated by 194 mm, except for some special regions such as the RF section. The apertures in the interaction regions are 84mm, therefore restricting to a maximum cavity envelope of below 150 mm.

As as short historical note, the first superconducting RF deflector was built by the joint collaboration of Karlsruhe and CERN in 1979. The RF separator operated at a frequency of 2.865 GHz and comprised of 104 cells to provide a deflecting voltage of approximately 2 MV/m. It was used at the CERN SPS to study unknown heavy particle, baryonic states and exchanges and provide particle species such as $K^{\pm}$ and $\bar{p}$ [7]. It is still in use at the U-70 experiment setup at IHEP at Protvino [8]. The first crab cavity (superconducting) was proposed and realized for the $e^{+} - e^{-}$ collider at KEKB in Japan. A very long R&D program leading to the successful construction and implementation of a 508.9 MHz crab cavity was carried out at KEKB [26]. The TM_{110} deflecting mode in a squased pillbox type cavity was chosen to provide a deflecting voltage of approximately 1.5 MV. A complex mechanism using a coxial type beam pipe coupler (see Fig. 9) was used to damp the both lower and higher order modes very strongly with a choke at the deflecting frequency. It was also used for tuning the tuning mechanism for the deflecting mode.

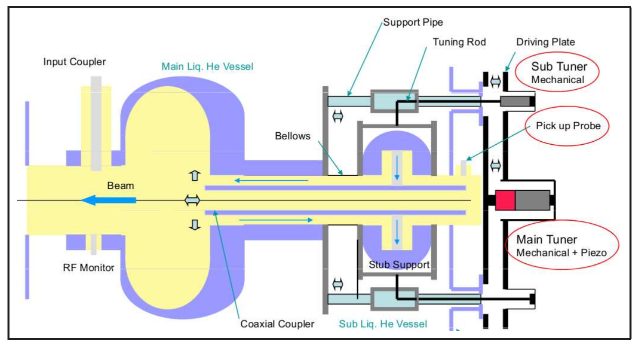

Figure 9: Longitudinal cross section of the KEKB crab cavity with the coaxial damping and tunind mechanism on the right side of the cavity.

Pillbox type for the LHC

As the first proposal a two cell elliptical cavity (pillbox type) was developed at SLAC (see Fig. 10) operating at 800 MHz [9]. Lower frequencies would make it impossible to fit within the LHC constraints. An extensive design study was carried out to develop compact and efficient lower and higher order mode couplers to meet the strict LHC impedance budget. Several aspects including multipacting, mechnical tolerances, cross coupling between couplers and thermal effects were studied in detail. In parallel, a single cell eccentric elliptical cavity (see Fig. 10) was also designed at 800 MHz with a single coupler to extract the lower and higher order modes [10]. The cavity is squashed strongly to fit within the IR regions of the LHC.

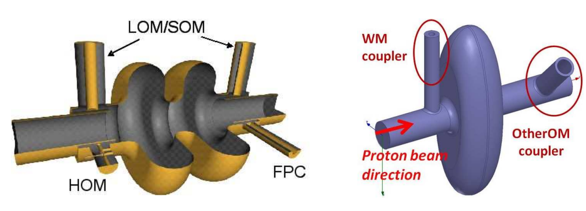

Figure 10: Left: The two-cell 800 MHz cavity design including all couplers. Right: Single-cell extremely squashed 800 MHz CERN design.

Even at 800 MHz, the primary drawback of both geometries is the transversal size. This leads to higher than desired frequencies and resort to eccentric elliptical profiles which can only fit in the interaction regions in a vertical crossing configuration. The LHC operates with a dual crossing scheme for passive compensation of long-range beam-beam effects. The higher RF frequency leads to RF non-linearity and consequent effects described in the previous section. In addition, the surface field ratio to the deflecting voltage is poor when compared to the accelerating TM_{010} mode.

TEM CLASS CAVITIES

Due to the limitations encountered with the standard pillbox geometries, an intensive R&D program was launched following the decision of the LHC-CC09 advisory committee to focus the development on compact designs at lower frequencies (400 MHz). An avalanche of conceptual designs immediately followed (see Fig. 11). The tight space constraints and the low frequencies pointed to TEM class resonators which are widely used in the heavy ion community at ultra low frequencies (<100 MHz). A detailed description of each cavity is out of the scope of this paper and only prospective designs at present at discussed.

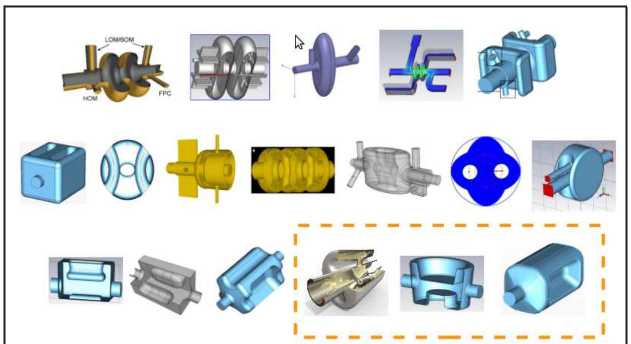

Figure 11: Schematics of the different geometried developed for the LHC crab cavities.

Quarter Wave

The simplest and perhaps the most compact transmission line cavity is the quarter wave resonator [11]. It consists of a coaxial geometry with an open at one end and a short at quarter of a wavelength from the open. At resonance, high voltage is generated between the two conductors at the open end which can used in different configurations (see Fig. 12) to interact with charged particles to accelerate of deflect the their trajectories.

The frequency of the quarter wave is principally dependent on the resonator length and weakly dependent on the gap or the radii of the concentric cylinders. The voltage developed between the resonator and the bottom plate can be used to deflect the particle trajectory with the integration path set perpendicular to the field. Despite the requirement of a large aperture, the asymmetrical structure of the quarter wave makes it is ideal for a small separation between the LHC beam pipes. The gap of the quarter wave can be

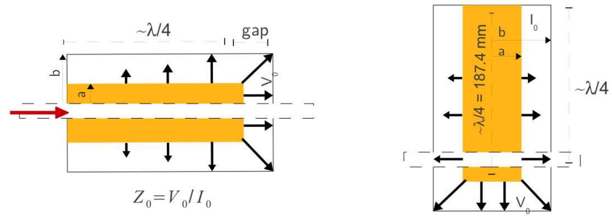

Figure 12: Quarter wave TEM line resonator

accomodated very easily for both horizontal or vertical deflections as shown in Fig. 13.

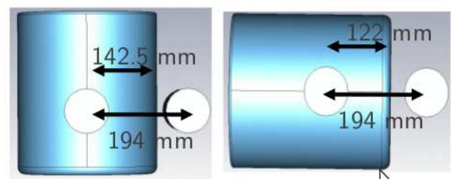

Figure 13: Quarter wave orientation for both horizontal and vertical deflections in the LHC IR region.

The primary advantage is that the operating mode is the first eigenmode of the resonator. For a pure quarter wave resonator, the next mode (first HOM) is located at 3 times the fundamental frequency. It should be noted that the design of the LHC crab cavity is only a quasi-quarter wave and separation is lower ($\times$1.5-2). A first proposal of 400 MHz design is shown in Fig. 15. Despite the quasi-quarter wave, the separation remains large between the operating mode and the higher order modes, thus making the HOM damping scheme simpler. For example, a high-pass filter is proposed as the choice of damper as opposed to notch filters for the LHC quarter wave for a robust performance.

The drawback of the quarter wave is a residual longitudinal electric field that results in a longitudinal voltage. For high beam currents, the beam loading on axis can become large and therefore requires a coupler and amplifier capable of high power. A simple remedy is an addition of a bottom pedestal (see Fig. 15) and careful adjustment of the lengths of the resonator and the pedestal can completely suppress the longitundal voltage on axis.

Half Wave

The next level to a quarter wave is a half wave TEM resonator. It can be thought of two quarter waves joined together in the appropriate configuration with both ends shorted with the length of the resonator at half the wavelength. At resonance, a high voltage is developed between the concentric cylinders at the central portion with the standing wave causing the voltage to travel as a consine and vanish at each end.

In its fundamental form, the half wave is most effective for acceleration. To deflect the particles, a higher order

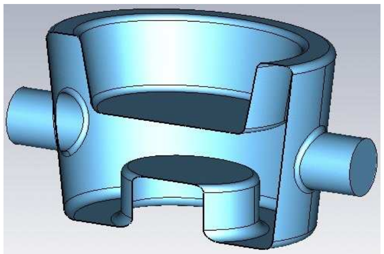

Figure 14: Schematic of a quarter wave resonator proposed for the LHC crab cavity.

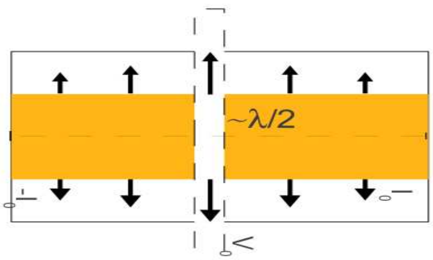

Figure 15: A half wave TEM resonator.

"TE_{11}-like" mode has to be employed (see Fig. 16). This was proposed and a detailed design for a 400 MHz LHC crab cavity was studied in great detail [13]. A more natural way to employ a half wave it to add an additional half wave resonator and use the voltage developed across the two TEM lines for particle deflection. This was first proposed for the CEBAF deflector and later adapted for the LHC at 400 MHz [14]. Although, half wave resonators can be made compact in the plane of deflection, the other plane is half a wavelength in dimension and therefore too big for vertical crossing configuration in the LHC interaction regions. To accomodate both crossing planes an improvement on the half wave concepts led to a simulataneous proposal of a double ridged waveguide by both the SLAC and the ODU groups (see Fig. 16). It should be noted that a double ridged waveguide structure was also initially proposed as a potential concept in 2008 [16].

Four Rod

A third type of a TEM class deflector is a 4-rod structure [17, 18] with two pairs of quarter waves placed in a co-linear configuration with the beam axis along the length of the resonators as shown in Fig. 17. Due to the 4-rod configuration, four eigenmodes at the fundamental "passband" are present of which only one mode is used for deflection. It should be noted that the deflecting mode is not the lowest order mode as in the case of a pillbox cavity. However, the TEM type cavity allows for an extremely compact transverse profile as the frequency is primarily dependent on the length of the 4-rods. A normal conducting version of a 4-rod deflector is already inn use in the CEBAF accelerator [19].

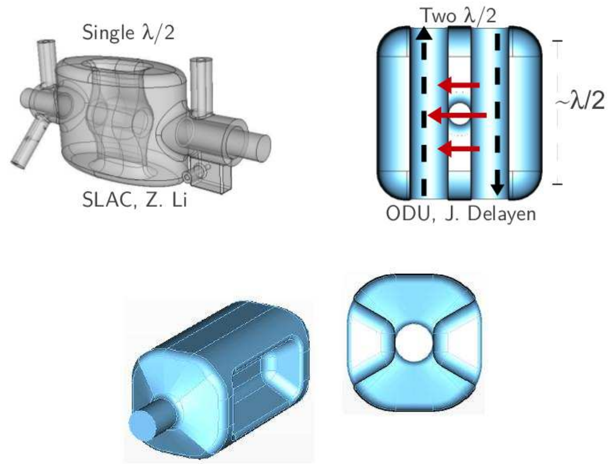

Figure 16: Top left: A SLAC half wave RF deflector at 400 MHz. Top right: A ODU-Jlab parallel bar RF deflector at 400 MHz. Bottom: ODU-SLAC double ridged structure as a deflector for the LHC crab scheme.

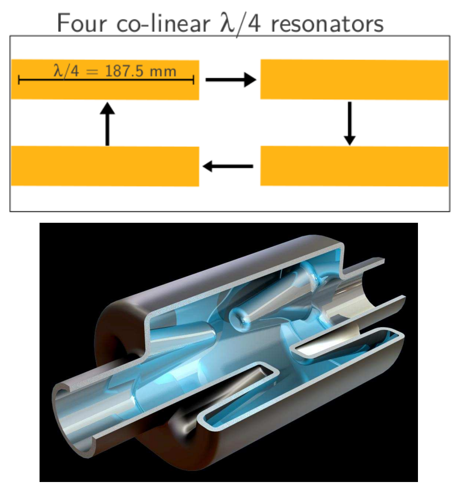

Figure 17: Top: Concept of the four colinear quarter wave resonators to form a RF deflector. Bottom: Schematic of the 4-rod LHC crab cavity at 400 MHz.

The rods are conical in shape for better mechanical stability and surface field distribution. In addition, some shaping of the rod along the beam axis is also performed to reduce the non-linear components of the deflecting field.

Cavity Comparison

The performance of the three TEM class resonators in their present form is listed in Table 3 into their geometrical compactness and peak surface fields at the operating voltage of 3 MV. It is important to note that all three cavities are atleast factor of 3 smaller than its elliptical counterpart at 400 MHz. The surface field to deflecting voltage ratio is also better despite the significant reduction of the size. This is a direct consequence of the TEM like mode where the fields are more evenly distributed along the resonator.

Table 3: Geometrical and RF parameter comparsion of the three TEM type deflectors for the LHC crab cavity at 400 MHz and 3 MV.

	Dbl Ridge ODU-SLAC	4-Rod LU-DL	$\frac{1}{4}$-Wave BNL
Cav Radius [mm]	147.5	143/118	142/122
Cav length [mm]	597	500	380
Aperture [mm]	84	84	84
E_{pk} [MV/m]	33	32	47
B_{pk} [mT]	56	60.5	71
$R_\perp/Q$ [Ω]	287	915	318
Next HOM [MHz]	584	317-378	575

OTHER ASPECTS

Beyond the cavity geometry and deflecting kick gradients, several other aspects of superconducting cavities are under investigation to validate a complete cryomodule for operational use in the LHC. Some pertinant topics affecting the cavity design including impedance, HOM damping, cavity noise, tuning and multipacting are addressed. The issue of machine protection in the event of a fast cavity failure is beyond the scope of this paper, but remains a critical issue under investigation. Mitigation techniques such as voltage distribution with two or more cavities, strong cavity to cavity feedback and adequate field margin are proposed and under investigation [20, 21, 22, 23].

Impedance Budget and HOM Damping

Impedance (both narrow band and broadband) from additional machine elements in the LHC like crab cavities need to be minimized to ensure beam stability along the LHC energy cycle. Tolerances can be set by estimating the impedance requirements from Refs. [24]. In a previous crab cavity workshop, these estimates were revised and updated tolerances were presented [25].

For the longitudinal plane, the impedance threshold is plotted as a frequency in Fig. 18 with a maximum allowed of 2.4 MΩ total from all cavities installed at 7 TeV. The frequencies of the first few longitudinal HOMs for the double ridged waveguide is also marked with arrows in Fig. **??**. For example assuming 8 cavities per beam at two IPs, the most dangerous mode with a R/Q = 200Ω the damping would required is approximately $Q_{ext} < 1.5 \times 10^3$. All other modes are atleast a factor 5 or more smaller. The damping schemes being considered aim at $Q_{ext} = 100 - 500$ is are well below the threshold.

For the transverse plane, the impedance budget is summarized in Table 4. For example, the strongest dipole mode in the double ridged structure is at 580 MHz. To damp

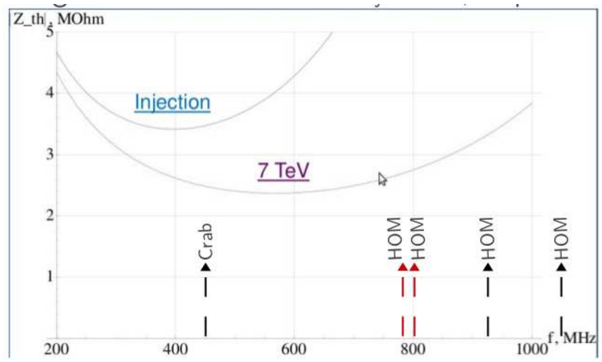

Figure 18: Longitundal impedance threshold as a function of frequency for injection and 7 TeV top energy [25].

this mode below the threshold of 0.75 MΩ/m (assuming 8 cavities per beam), the required $Q_{ext} < 600$. The present damping concepts already aim at values well below this. A damping time $\tau_d = 60$ms is assumed from the bunch-by-bunch transverse feedback system. Also, note that this assumes a pessimistic case that the frequency of a particular HOM in all cavities remain same and the beam harmonic conincides with the HOM frequency. The natural HOM frequency spread, chromaticity, improved damping time, and Landau octupoles should also alleviate these requirements. HOMs at higher frequencies should be Landau-damped due to the frequency spread of synchrotron oscillations.

Table 4: Transverse impedance thresholds at injection and 7 TeV top energy to ensure beam stability using 4 cavities per beam [25].

Energy	β_{crab}	Impedance, -Re$\{Z_{th}\}$
450 GeV	150 m	2.7 MΩ/m
7 TeV	4000 m	1.5 MΩ/m

Damping and Frequency Tuning

Based on the impedance tolerances, a cavity specific damping scheme is being developed for each of the three designs (see Fig. 19). The quarter wave and ridged resonators have the deflecting mode as the fundamental mode by design. In addition these cavities have the property of large separation ($>$ 150 MHz) between the operating mode and the HOMs. This uniquely lends itself to the use of high-pass filters to damp the HOMs strongly while robustly rejecting the operating mode. A high pass filter design developed for a 56 MHz resonator (see Fig. 19) will be adapted to 400 MHz for the quarter wave. For the double ridged cavity, four symmetry coaxial couplers with symmetry on the beam axis is proposed [15]. The exact design of the HOM couplers is under study. The 4-rod design, due to the four eigenmodes in proimity, has to use targeted couplers for lower and higher order modes like in the elliptical cavities. No notch filter to reject the operating mode is presently proposed, but may become necessary to avoid extracting excessive operating mode power into the HOM couplers due to asymmetries or fabrication errors. A detailed damping concept for each cavity is being developed. First results show damping values well below the impedance thresholds.

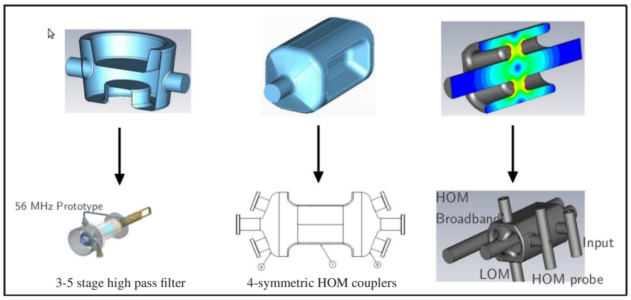

Figure 19: Schematic of the proposed damping concepts for the three TEM type deflecting resonators [15, 18].

RF Noise

Amplitude or cavity voltage jitter introduces a residual crossing angle at the IP proportional to the error (see Fig. 20). It is sufficient that this residual crossing angle is much smaller (<1%) than the geometric angle leading to a tolerance of [26]

$$\frac{\Delta V_{\perp}}{V_{\perp}} \ll \frac{1}{\tan(\theta_c/2)} \frac{\sigma_x^*}{\sigma_z}. \tag{6}$$

Alternatively, a phase error in the RF wave causes an offset of the bunch rotation axis translating into a transverse offset at the IP as shown in Fig. 20. The offset at the IP is given by

$$\Delta x_{IP} = \frac{c\theta_c}{\omega_{RF}} \, \delta\phi_{RF} \tag{7}$$

where θ_c is the full crossing angle and $\delta\phi_{RF}$ is the phase error. Random kicks from the crab cavity and offsets at the IP coupled with beam-beam can lead to emittance growth which is of main concern for Hadrons.

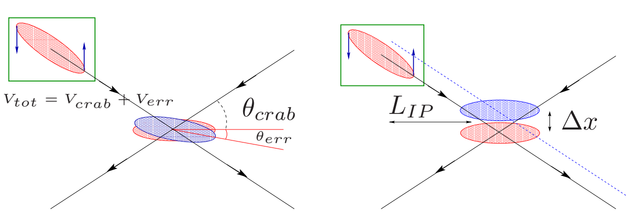

Figure 20: Left: Schematic of cavity voltage error leading to a residual crossing angle at the IP. Right: RF phase jitter resulting in a transverse offset at the IP.

Using the upgrade crossing angle of approximately $\theta_c = 570\mu$rad, $\sigma^* = 7\mu$m and nominal bunch length, a voltage error of $\Delta V/V$ of 0.4% introduces a residual crossing angle of only 1.2 μrad. Low level RF systems in the LHC should be able to control the voltage jitter to 0.1% or lower leading to negligible effects.

Using the phase jitter summed up at all betatron band from DC to 300 kHZ measured in the main RF cavities in the LHC, a phase jitter of about $\Delta\phi = 0.005°$ can be expected with the prsent LLRF system [23]. This jitter for upgrade parameters lead to an IP offset of $\Delta x_{IP} = 0.3\mu$m which is approximately 5% of the transverse beam size. Weak-strong and strong-strong simulations indicate a phase jitter tolerance between 0.001°-0.01° [27] and is inversly proportional to the noise correlation time. The crab cavities will nominally use IOTs or solid state power sources which have inherently better noise characteristics than klystrons that are used for the LHC main RF cavities. Additional filters such as the betatron combs will reduce the noise levels at specified band well below 1×10^{-3} deg if required.

Multipacting

Multipacting is of general concern in TEM type geometries. This phenomena occurs due to resonant electron multiplication of electrons emitted from the cavity surface and impacting back thereafter in integer number of RF cycles. If the secondary electron yeild (SEY) of the surface is greater than 1, this can lead to an avalanche, and possibly a thermal breakdown of superconducting surfaces. 3D particle tracking codes [28] are used to investigate electron trajectories at various field levels with appropriate SEY for the surface. Fig. 21 shows three different types of multipacting [18, 15]:

- Low field multipacting both for 4-rod and double ridged cavities primarily in the equator region and distributed along the resonator length. These trajectories are either weak or moderate.
- String multipacting is observed in the beam pipe region for both designs, similar to the KEKB elliptical cavity.
- Very weak multipacting is also observed in the double ridged structure in the central part of the equator.

All of the above multipacting can be suppressed with RF processing of the cavity surface. Strong multipacting like in the moderate field region may increase this processing time. Small ridges can also be used on the beam pipes to geometrically suppress the multipacting if needed. For the quarter wave, the multipacting is generally well know and usually RF processing is sufficient to suppress it. For the specific deflector geometry, studies are ongoing to identify the different orders and field levels and their respective strengths.

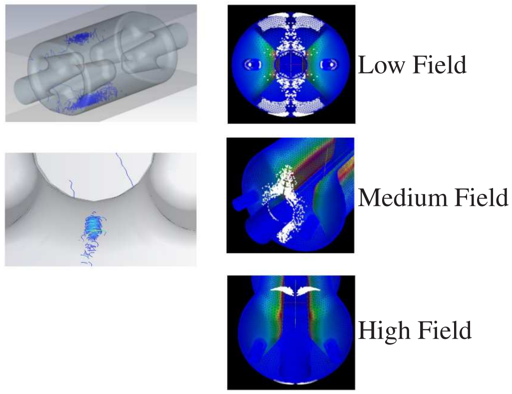

Figure 21: Multipacing trajectories at different voltage regimes for the 4-rod and the double ridged structure.

PLANNING & PROTOTYPES

The planning for a final crab cavity system is evolving with the latest developments and the overall LHC operational schedule. A detailed planning for the crab system in the context of the HL-LHC is described in Ref. [29]. The overall planning will progress in approximately three stages. The first stage (ongoing) will focus primarily on the validation of the cavity design. During this period (2012-13), prototypes of the three cavities will be built for a field validation in a vertical test configuration inside a 2K Helium bath.

For the first stage, prototypes of the 4-rod and the double ridge cavities have advanced rapidly. An aluminum structure of the 4-rod has been built for field and HOM measurements which have been successfully carried out (see Fig. 22). The first Niobium model was completed in Feb 2012 and warm measurements are underway. Preparations for measurements at 2K will follow and will likely take place in the next months.

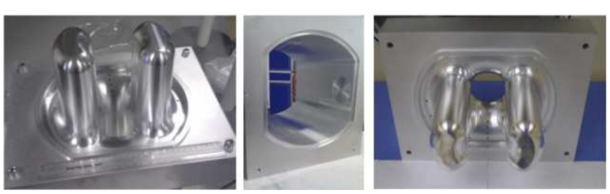

Figure 22: Pictures of the first Aluminum prototype cavity of the 4-rod structure.

The double ridge structure evolved from an earlier parallel bar deflector which under a STTR program was approved for fabrication. Successful tests on an Aluminum model have been performed in 2011. The Niobium model was fabricated based on the latest double ridge design in late 2011. Fig. 23 illustrates the fabrication steps resulting into a final cavity which is being assembled for testing at 2K. It should be noted that the design has slightly evolved into a square topology for further compactness since the start of the fabrication in late 2011. This will however not affect the conclusions of the 2K tests of the bare cavity which will take place in April 2012.

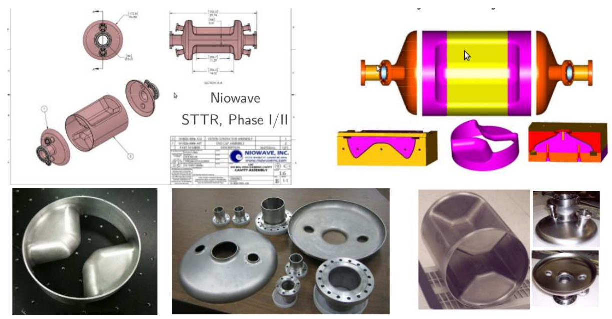

Figure 23: Top: Engineering drawing and fabrication concept for the double ridged structure. Bottom: Pictures of the first Niobium prototype cavity.

The RF design of the quarter wave cavity is being finalized. The fabrication of either a copper or a Niobium model will imemdiately follow with the goal of testing the cavity in early 2013.

Following the successful cavity tests, the second stage will dress the cavity into a complete cryomodule with couplers and ancilliary equipment. A prototype cryomodule consisting of atleast one cavity is foreseen to be tested in the SPS and or the LHC for a validation with proton beams [30]. These tests should take place after LS1 shutdown and prior to LS2 shutdown [29]. A production phase for the complete crab system consisting of four modules per IP with 2-3 cavities per modules will follow a successful demonstration with beam using a the prototype cryomodule.

ACKNOWLEDGMENTS

The author would like to thank all the members of LHC-CC collaboration for valuable contributions and discussions. The author would also like to extend a special thanks to E. Ciapala, E. Jensen, R. Tomas and F. Zimmermann.

REFERENCES

[1] G. Papotti et al., Observation of bunch by bunch differences due to beam-beam effects, CERN-ATS-2011-217, CERN, 2011.

[2] S. White et al., Synchro-Betatron Effects, LHC-CC11, CERN, 2011.

[3] R. Palmer, Energy scaling, crab crossing and the pair problem SLAC-PUB-4707, 1988

[4] R. de Maria et al., Upgrade optics with crab cavities, LHC-CC10, CERN, Geneva, 2010.

[5] Y. Sun et al., Phys. Rev. ST Accel. Beams 12, 101002 (2009).

[6] E. Montesinos, private communication.

[7] A Citron et al., The Karlsruhe - CERN superconducting rf separator, NIM, Vol. 164-1, 1979.

[8] OKA experimental program, IHEP, Protvino.

[9] Z. Li et al., LHC-CC09, CERN, 2009.

[10] L. Ficcadenti et al., Slim elliptical cavity at 800 MHz for local crab crossing, LHC-CC10, CERN, 2010.

[11] I. Ben-Zvi, J. Brennan, NIMA, A212, 73, 1983.

[12] I. Ben-Zvi, Quarter wave resonators for high-β accelerators, SRF2011, Chicago, 2011.

[13] Z. Li et al., LARP cavity developments, LHC-CC10, CERN, Geneva, 2010.

[14] J. Delayen, H. Wang, Phys. Rev. ST Accel. Beams 12, 062002 (2009).

[15] J. Delayen et al., USLARP-CM16, Montauk, NY, 2011.

[16] F. Caspers, LHC crab cavity validation workshop, CERN, Geneva, 2008.

[17] G. Burt et al., UK R&D for LHC crab cavities, LHC-CC09, CERN. Geneva, 2009.

[18] B. Hall et al., 4 rod RF design, LHC-CC11, CERN. Geneva, 2011.

[19] H. Wang et al., LHC-CC08, BNL, NY, 2008.

[20] R. Calaga et al., LHC Crab Cavities, LHC performance workshop, Chamonix, 2010.

[21] R. Calaga et al., Beam losses due to abrupt crab cavity failures in the LHCPAC11, New York, 2011.

[22] T. Baer et al., Machine protection simulations, LHC-CC11, CERN, Geneva, 2011.

[23] P. Baudrenghien et al., Running the RF at higher beam energy and intensity, LHC performance workshop, Chamonix, 2012.

[24] E. Shaposhnikova, LHC Project Note 242 (2000); F. Sacherer, IEEE Tr. Nucl.Sci. NS-20 , 825 (1973); V. Balbekov et al., IHEP Preprint 91-14, Protvino (1991).

[25] A. Burov et al., Impedance Aspects, LHC-CC11, CERN, Geneva, 2011.

[26] K. Oide, K. Yokoya, Physical Review A, 40, 315 (1989).

[27] K. Ohmi, Beam-beam effect with an external noise in LHC, PAC07, Knoxville, TN, 2007.

[28] L. -Q .Lee, et al., SLAC-PUB-13529, 2009.

[29] E. Jensen, HL-LHC and Crab cavity planning, LHC-CC11, CERN, Geneva, 2011.

[30] R. Calaga et al, SPS beam studies, LHC-CC11, CERN, Geneva, 2011.